Preprints of the 19th World Congress
The International Federation of Automatic Control
Cape Town, South Africa. August 24-29, 2014

Feed-forward control of a vehicle with single-wheel actuators

Jan-Erik Moseberg * **Günter Roppenecker** *

* *Lehrstuhl für Regelungstechnik*
Friedrich-Alexander Universität Erlangen-Nürnberg
Cauerstr. 7, 91058 Erlangen, Germany
jan-erik.moseberg@fau.de

Abstract: For the horizontal motion of a vehicle with single-wheel actuators a model-based feed-forward control is derived. Using the accelerator and brake pedal position as well as the steering wheel angle, the feed-forward control generates a desired vehicle motion together with appropriate longitudinal and lateral forces on the vehicle mass and a corresponding yaw moment. Since no detailed vehicle model, e.g., the single-track model, is required it is possible to tune the horizontal vehicle dynamics arbitrarily without changing the vehicle's geometry. Subsequently, the obtained forces and the yaw moment are allocated to the eight horizontal tire forces. Since the vehicle considered is over-actuated a secondary objective, i.e., the safety maximization, can be pursued in addition to realizing the desired vehicle motion. Solving this optimization problem numerically in a real vehicle is time-critical, so an analytical solution is introduced.

Keywords: Vehicle dynamic systems; Nonlinear and optimal automotive control; Control architectures in automotive control.

1. INTRODUCTION

This article presents a feed-forward control structure for the horizontal motion of a vehicle with single-wheel actuators, i.e., single-wheel steering, brake, and drive. Since such a vehicle is an over-actuated system with redundant actuators it is possible to adapt the tire forces of each single wheel independently. Moreover, there are additional degrees of freedom that can be used to pursue secondary objectives in addition to achieving a desired plane vehicle motion [1, 2]. While most articles dealing with this topic focus on force allocation [3] and feedback control [4], this paper also takes the generation of adequate trajectories for the desired vehicle motion into account.

On the basis of a simple model for the longitudinal, lateral, and yaw dynamics of the vehicle body, driven by the eight tire forces, a feed-forward control structure is developed. Using the brake and accelerator pedal position plus the steering wheel angle as inputs, the feed-forward control generates a desired vehicle motion as well as corresponding forces and moments on the vehicle chassis. Unlike using a more detailed vehicle model, e.g., a single-track model, for generation of the desired vehicle motion, here the correlations between the driver's request and the resulting vehicle motion can be parameterized freely.

Subsequently, the desired forces and the yaw moment on the vehicle chassis are allocated to the eight horizontal tire forces. Thereby the redundant actuators are used to pursue a maximum in driving safety in addition to realizing the desired vehicle motion. Since solving the underlying optimization problem in a real vehicle is time-critical an approach to allocate the tire forces by analytically minimizing an appropriate cost function is presented.

This paper is structured as follows: In Sec. 2 the required vehicle model is derived. Based on this model an appropriate design of the feed-forward control for the vehicle's horizontal dynamics will be carried out in Sec. 3. The following section deals with the analytical force allocation. In Sec. 5 the designed feed-forward control is validated in comparison with the single-track vehicle model. Furthermore, the efficiency of the designed force allocation concerning the safety maximization is demonstrated by simulating a highly dynamic driving maneuver.

2. VEHICLE MODEL

The derivation of the feed-forward control is based on a simple two-track vehicle model describing the main characteristics of the longitudinal, lateral, and yaw motion of a vehicle whose tire forces can be adapted individually, e.g., a vehicle with single-wheel actuators. Vertical effects and aerodynamic influences are not to be considered.

Assuming that the vehicle behaves like a rigid body moving on a plane road its horizontal motion is determined by the eight independently adjustable tire forces $\underline{F}_{xy} = [\, F_{x1} F_{y1} \ldots F_{x4} F_{y4} \,]^T$. With respect to the vehicle's dimensions (cf. Fig. 1) the tire forces can be summarized by the longitudinal and lateral forces F_x and F_y, and the yaw moment M_z acting on the vehicle's center of gravity:

$$\underline{F}_H = \underbrace{\begin{bmatrix} 1 & 0 & 1 & 0 & 1 & 0 & 1 & 0 \\ 0 & 1 & 0 & 1 & 0 & 1 & 0 & 1 \\ -s_l & l_v & s_r & l_v & -s_l & -l_h & s_r & -l_h \end{bmatrix}}_{\underline{\underline{G}}} \underline{F}_{xy}. \qquad (1)$$

In order to obtain a horizontal vehicle model a vehicle-fixed coordinate system with the basis vectors $\underline{e}_x$ and $\underline{e}_y$

Copyright © 2014 IFAC

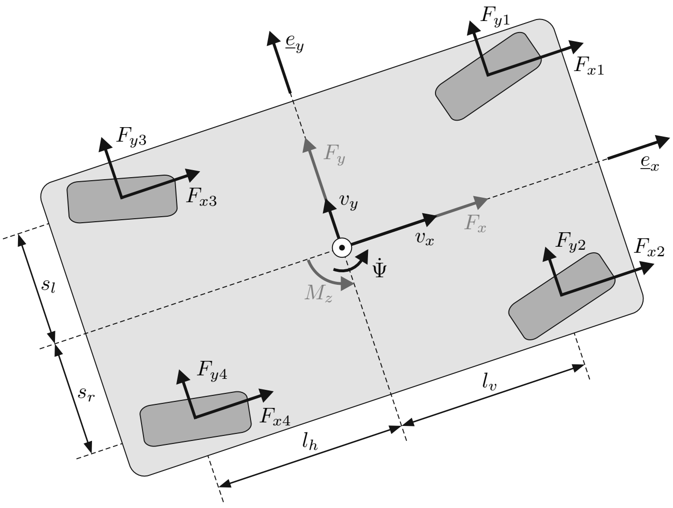

Fig. 1. Depiction of the horizontal vehicle motion.

is introduced. Since the vehicle rotates relative to a road-fixed inertial system with the yaw rate $\dot{\Psi}$ about its vertical axis the longitudinal and lateral accelerations a_x and a_y of the vehicle's center of gravity read

$$a_x = \dot{v}_x - v_y \dot{\Psi}, \quad a_y = \dot{v}_y + v_x \dot{\Psi} \tag{2}$$

with $v_x > 0$ and v_y being the vehicle's longitudinal and lateral velocity in the vehicle-fixed coordinate system. Thus the basic equations of the horizontal vehicle motion result from the principles of impulse and momentum with the vehicle's mass m and its yaw moment of inertia J_z:

$$\frac{\mathrm{d}}{\mathrm{d}t} \underbrace{\begin{bmatrix} v_x \\ v_y \\ \dot{\Psi} \end{bmatrix}}_{\underline{v}_H} = \begin{bmatrix} v_y \dot{\Psi} \\ -v_x \dot{\Psi} \\ 0 \end{bmatrix} + \begin{bmatrix} \frac{1}{m} & 0 & 0 \\ 0 & \frac{1}{m} & 0 \\ 0 & 0 & \frac{1}{J_z} \end{bmatrix} \underbrace{\begin{bmatrix} F_x \\ F_y \\ M_z \end{bmatrix}}_{\underline{F}_H}. \tag{3}$$

The output variables read $\underline{y}_H = \begin{bmatrix} a_x & a_y & \dot{\Psi} \end{bmatrix}^T$.

3. FEED-FORWARD CONTROL STRUCTURE FOR THE VEHICLE'S HORIZONTAL DYNAMICS

Based on the developed system description for the horizontal vehicle dynamics (3) a feed-forward control structure determining a desired horizontal vehicle motion $\underline{y}_{H,d}$ and appendant forces and moments $\underline{F}_{H,d}$ on the vehicle chassis is derived in this section. First, desired forces on the vehicle's center of gravity are generated with regard to the driver's request characterized by brake and accelerator pedal position as well as steering wheel angle. By controlling a model of the vehicle's horizontal dynamics a consistent yaw moment together with a desired vehicle motion are obtained.

3.1 Generation of the longitudinal and lateral forces

Operating the accelerator pedal and the brake pedal, the driver determines a longitudinal force $F_{x,d}$ on the vehicle chassis such that the desired longitudinal velocity results despite the driving resistances. In the considered feed-forward control structure the desired longitudinal force $F_{x,d}$ is a proportion of a physically maximum force $F_{x,max}$ that depends on the vehicle's drive and brake system:

$$F_{x,d} = k(\alpha_{a/b})\ F_{x,max}. \tag{4}$$

With the characteristic $k(\alpha_{a/b})$ the correlation between the longitudinal force $F_{x,d}$ and the pedal positions α_a or α_b respectively can be parameterized. Linear, progressive, or degressive dependencies are conceivable, for instance.

In addition the driver determines a desired lateral force $F_{y,d}$ on the vehicle chassis operating the steering wheel. In the presented feed-forward control structure this lateral force is generated in such a way that a desired self-steering behavior results. Therefore the vehicle is assumed to act like a point mass m moving at the longitudinal velocity $v_{x,d}$ along a trajectory with radius r around the instantaneous center of curvature P (cf. Fig. 2). To maintain its trajectory the vehicle requires the centripetal force $F_{y,d}$ that is proportional to the vehicle's mass m, the square of its longitudinal velocity $v_{x,d}^2$, and the trajectory's curvature $\kappa_d = \frac{1}{r}$:

$$F_{y,d} = \kappa_d\ m\ v_{x,d}^2. \tag{5}$$

The determination of the curvature κ_d is based on the required steering wheel angle performing a steady-state circular test (see e.g. [5]):

$$\delta_{sw} = i_s \left(l + \mathrm{EG}\ v_x^2 \right)\ \kappa \tag{6}$$

with the vehicle's wheelbase $l = l_v + l_h$, the steering ratio i_s, and the self-steering gradient EG. Rearranging (6) yields the desired curvature:

$$\kappa_d = \left(\nu + \mathrm{EG}_d\ v_{x,d}^2 \right)^{-1} k(\delta_{sw}). \tag{7}$$

The parameters ν and EG_d determine the desired self-steering behavior; the steering response depends on the arbitrarily tunable characteristic $k(\delta_{sw})$.

3.2 Determination of a consistent yaw moment

The horizontal vehicle motion not only depends on the longitudinal and lateral forces on the chassis but also on the yaw moment. Thus the feed-forward control structure is extended by a controlled model of the vehicle's horizontal dynamics generating a consistent yaw moment that additionally ensures a desired stationary sideslip angle behavior. The sideslip angle

$$\beta = \arctan \left(\frac{v_y}{v_x} \right) \tag{8}$$

denotes the angle between the vehicle's longitudinal axis and the moving direction of its center of gravity.

The associated control law results from the horizontal vehicle dynamics according to (3) considering the yaw moment as input $u = M_{z,d}$ and the lateral velocity as output $y = v_{y,d}$. In order to track a reference output signal w an exact input-output linearization of the nonlinear system is implemented. The resulting linear and controllable

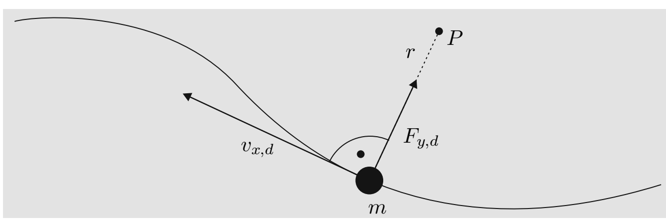

Fig. 2. Modeling the vehicle as a point mass

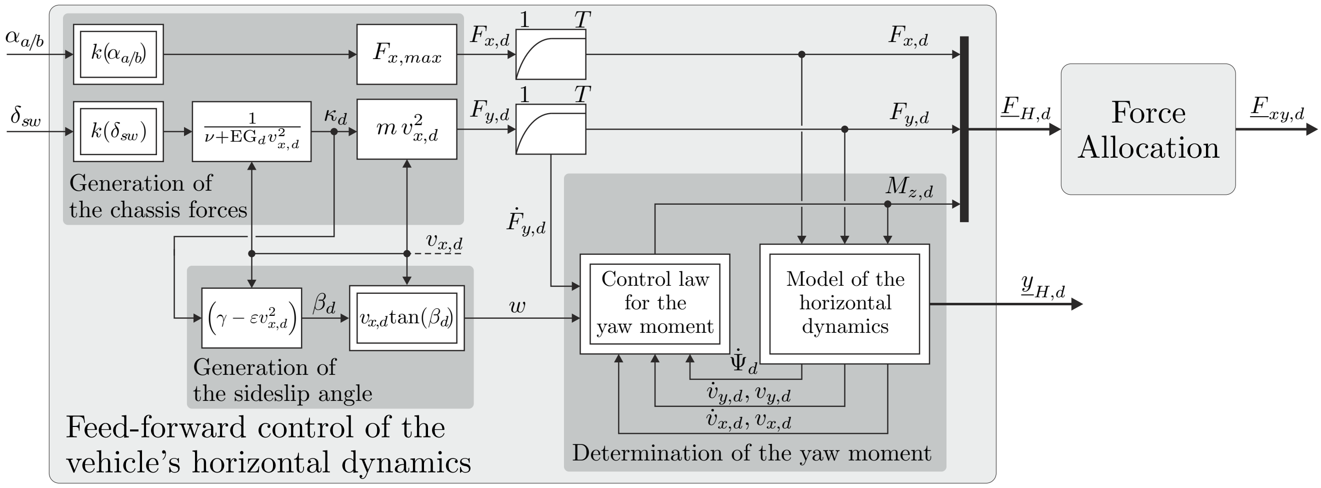

Fig. 3. Feed-forward control structure for the vehicle's horizontal dynamics

integrator chain is stabilized by state feedback. With the coefficients $a_0, a_1 > 0$ reflecting the desired transmission behavior the control law reads:

$$M_{z,d} = \frac{J_z}{v_{x,d}}\left(-\dot{v}_{x,d}\dot{\Psi}_d + \frac{\dot{F}_{y,d}}{m} + a_1\dot{v}_{y,d} + a_0 v_{y,d} - a_0 w\right). \quad (9)$$

Since the relative degree $r = 2$ of the considered system is less than its order $n = 3$ applying the input (9) yields a zero dynamics of first order. However, the stability of the closed loop system can be guaranteed because of the given stability of the zero dynamics.

Rearranging the sideslip angle definition (8) results in the reference output signal

$$w = v_{x,d} \tan \beta_d. \quad (10)$$

The determination of the sideslip angle β_d is based on the stationary sideslip angle of a conventional vehicle

$$\beta = \left(l_h - \frac{m}{c_{\alpha r}}\frac{l_v}{l_v + l_h}v_x^2\right)\kappa \quad (11)$$

with $c_{\alpha r}$ being the rear wheel's cornering stiffness (see e.g. [5]). Introducing the general parameters γ and ε the desired sideslip angle reads

$$\beta_d = \left(\gamma - \varepsilon\, v_{x,d}^2\right)\kappa_d. \quad (12)$$

By tuning the parameters γ and ε it is possible to freely choose the stationary sideslip angle behavior. For example, a stationary sideslip angle $\beta_d = 0$ can easily be implemented by $\gamma = \varepsilon = 0$.

3.3 Resulting feed-forward control structure

Figure 3 shows the resulting feed-forward control structure for the vehicle's horizontal dynamics. Utilizing the accelerator or brake pedal position respectively and the steering wheel angle, a longitudinal and a lateral force on the vehicle chassis are generated. Furthermore, it is possible to realize a desired self-steering behavior. A consistent yaw moment is the result of a controlled model of the vehicle's horizontal dynamics leading to a desired stationary sideslip angle. Since the derivative $\dot{F}_{y,d}$ occurs in the related control law (9) a first-order low pass filter with time constant T and gain 1 is necessary. To ensure a similar response characteristic concerning the longitudinal vehicle motion such a filter is used in the $F_{x,d}$-path, too.

Next the desired longitudinal and lateral forces as well as the yaw moment summarized in $\underline{F}_{H,d}$ are allocated to eight desired tire forces $\underline{F}_{xy,d}$. Furthermore, the horizontal motion trajectory $\underline{y}_{H,d}$ generated in the model of the horizontal vehicle dynamics is fed forward to an additional chassis control loop that is not part of this article [6].

4. TIRE FORCE ALLOCATION

In order to realize the forces and moments $\underline{F}_{H,d}$ on the vehicle chassis appropriate tire forces $\underline{F}_{xy,d}$ have to be created. The required tire force allocation follows from the general solution of (1) exploiting the over-actuation of the system to achieve a maximum in driving safety by analytically minimizing a cost function J. Since matrix $\underline{\underline{G}} \in \mathbb{R}^{3\times 8}$ is of full row rank the general solution of (1):

$$\underline{F}_{xy,d} = \underline{\underline{G}}^{+}\underline{F}_{H,d} + \underline{\underline{G}}^{\perp}\underline{\Delta F}_{xy} \quad (13)$$

is obtained utilizing the Moore-Penrose inverse and a kernel of $\underline{\underline{G}}$ (see e.g. [7]):

$$\underline{\underline{G}}^{+} = \underline{\underline{G}}^{T}\left(\underline{\underline{G}}\,\underline{\underline{G}}^{T}\right)^{-1}, \quad (14)$$

$$\underline{\underline{G}}^{\perp} = \ker\left(\underline{\underline{G}}\right). \quad (15)$$

The resulting vehicle motion is unaffected by the arbitrary force parameters $\underline{\Delta F}_{xy}$ having no influence on $\underline{F}_{H}$, i.e., the longitudinal and lateral forces and the yaw moment. However, the force parameters do affect the allocation of the longitudinal and lateral tire forces $\underline{F}_{xy,d}$. Thus it is possible to pursue the objective of safety maximization in addition to realizing the desired vehicle motion.

Driving safety strongly depends on each tire's utilization of adhesion potential

$$\eta_i = \frac{\|\underline{F}_i\|}{F_{\mathrm{max}i}}, \quad i = 1\ldots 4 \quad (16)$$

determined by the force vector $\underline{F}_i = \left[F_{xi}\ F_{yi}\right]^T$ summarizing the longitudinal and lateral tire forces F_{xi} and F_{yi} as well as by the adhesion limit $F_{\mathrm{max}i}$ depending on the wheel load and the friction in between tire and ground. Thus a weighted square sum of the four utilizations $\eta_{i,d}$ is chosen as cost function:

$$J = \sum_{i=1}^{4} q_i \eta_{i,d}^2 = \sum_{i=1}^{4} q_i \frac{F_{xi,d}^2 + F_{yi,d}^2}{F_{\max i,d}^2}. \tag{17}$$

Introducing the positive definite weighting matrix $\underline{\underline{Q}} \in \mathbb{R}^{8\times 8}$:

$$\underline{\underline{Q}} = \begin{bmatrix} \frac{q_1}{F_{\max 1,d}^2} & 0 & \cdots & 0 & 0 \\ 0 & \frac{q_1}{F_{\max 1,d}^2} & & & 0 \\ \vdots & & \ddots & & \vdots \\ 0 & & & \frac{q_4}{F_{\max 4,d}^2} & 0 \\ 0 & 0 & \cdots & 0 & \frac{q_4}{F_{\max 4,d}^2} \end{bmatrix} \tag{18}$$

and substituting (13) in (17) the cost function J reads:

$$\begin{aligned} J &= \underline{F}_{xy,d}^T \, \underline{\underline{Q}} \, \underline{F}_{xy,d} \\ &= \left(\underline{F}_{H,d}^T \, \underline{\underline{G}}^{+T} + \underline{\Delta F}_{xy}^T \, \underline{\underline{G}}^{\perp T}\right) \underline{\underline{Q}} \left(\underline{\underline{G}}^{+} \underline{F}_{H,d} + \underline{\underline{G}}^{\perp} \underline{\Delta F}_{xy}\right) \\ &= \underline{F}_{H,d}^T \, \underline{\underline{G}}^{+T} \underline{\underline{Q}} \, \underline{\underline{G}}^{+} \underline{F}_{H,d} + \underline{F}_{H,d}^T \, \underline{\underline{G}}^{+T} \underline{\underline{Q}} \, \underline{\underline{G}}^{\perp} \underline{\Delta F}_{xy} \\ &\quad + \underline{\Delta F}_{xy}^T \, \underline{\underline{G}}^{\perp T} \underline{\underline{Q}} \, \underline{\underline{G}}^{+} \underline{F}_{H,d} + \underline{\Delta F}_{xy}^T \, \underline{\underline{G}}^{\perp T} \underline{\underline{Q}} \, \underline{\underline{G}}^{\perp} \underline{\Delta F}_{xy}. \end{aligned} \tag{19}$$

The arbitrary parameters $\underline{\Delta F}_{xy}$ are to be chosen in such a way that the cost function J is minimized. This objective is achieved through zeroing the gradient of J with respect to the force parameters $\underline{\Delta F}_{xy}$ and solving for $\underline{\Delta F}_{xy}$:

$$\begin{aligned} \frac{\partial J}{\partial \underline{\Delta F}_{xy}} &= 2\, \underline{F}_{H,d}^T \, \underline{\underline{G}}^{+T} \underline{\underline{Q}} \, \underline{\underline{G}}^{\perp} + 2 \underline{\Delta F}_{xy}^T \, \underline{\underline{G}}^{\perp T} \underline{\underline{Q}} \, \underline{\underline{G}}^{\perp} \stackrel{!}{=} \underline{0}^T \\ \Leftrightarrow \; \underline{\Delta F}_{xy}^{\min} &= -\left[\underline{\underline{G}}^{\perp T} \underline{\underline{Q}} \, \underline{\underline{G}}^{\perp}\right]^{-1} \underline{\underline{G}}^{\perp T} \underline{\underline{Q}} \, \underline{\underline{G}}^{+} \underline{F}_{H,d}. \end{aligned} \tag{20}$$

By calculating the Hessian matrix of J it can be demonstrated that the extremum obtained by the force parameters $\underline{\Delta F}_{xy}^{\min}$ in fact is a minimum of the cost function.

The weighting coefficients' influence on driving safety is investigated in [8]. There it is shown that choosing q_i as:

$$q_i = F_{\max i,d} \tag{21}$$

approximates the minimum of the maximum value of the four utilizations of adhesion potential

$$\eta_{\max} = \max_{i=1\ldots 4} \eta_i. \tag{22}$$

Hence, compared to any other examined choices of q_i, the utmost driving safety is achieved.

At last, the required tire forces $\underline{F}_{xy,d}$ result from substituting $\underline{\Delta F}_{xy}^{\min}$ in (13). Underlying single-wheel controllers which are not further discussed here realize the desired tire forces by adjusting rotational speed and steer angle at each single wheel [6].

5. SIMULATION RESULTS

In this section the benefit of the presented control structure will be investigated. First, the feed-forward control for the vehicle's horizontal dynamics according to Sec. 3 is compared to a reference model frequently used for generating trajectories for the horizontal vehicle motion. Subsequently, the effectiveness of the tire force allocation derived in Sec. 4 is demonstrated in comparison with an optimization based distribution of the tire forces.

5.1 Assessment of the horizontal dynamics' feed-forward control structure

The resulting feed-forward control structure's capability to generate adequate trajectories for the desired vehicle motion is evaluated by comparing its lateral dynamics behavior to the one of a conventional vehicle described by the well-known single-track vehicle model. Therefore their frequency and step responses resulting from an excitation by the steering wheel angle are examined. Assuming a constant longitudinal velocity $v_{x,d}$ as well as a small sideslip angle leading to $\tan(\beta) = \beta$ the required transfer functions are obtained. Furthermore, a linear characteristic $k(\delta_{sw}) = k_\delta \delta_{sw}$ is used. Thus the transfer functions of the feed-forward control read for the lateral acceleration:

$$G_{a_y}(s) = \frac{k_\delta v_{x,d}^2}{\nu + \mathrm{EG}_d v_{x,d}^2} \cdot \frac{1}{1+Ts}, \tag{23}$$

for the sideslip angle:

$$G_\beta(s) = \frac{k_\delta \left(\gamma - \varepsilon v_{x,d}^2\right)}{\nu + \mathrm{EG}_d v_{x,d}^2} \cdot \frac{a_0}{s^2 + a_1 s + a_0}, \tag{24}$$

and for the yaw rate:

$$G_{\dot\Psi}(s) = \frac{k_\delta}{\nu + \mathrm{EG}_d v_{x,d}^2} \cdot \frac{b_{\dot\Psi 2} s^2 + b_{\dot\Psi 1} s + b_{\dot\Psi 0}}{(s^2 + a_1 s + a_0)(1+Ts)} \tag{25}$$

where:

$$b_{\dot\Psi 2} = v_{x,d} - a_0 T \left(\gamma - \varepsilon v_{x,d}^2\right), \tag{26}$$

$$b_{\dot\Psi 1} = a_1 v_{x,d} - a_0 \left(\gamma - \varepsilon v_{x,d}^2\right), \tag{27}$$

$$b_{\dot\Psi 0} = a_0 v_{x,d}. \tag{28}$$

The corresponding transfer functions of the single-track vehicle model can be found in [5]. To achieve comparability of results the free parameters in (23), (24), and (25) are determined in accordance with the corresponding parameters of the compared single-track vehicle model (see Table 1). The specification of a_0, a_1, and T provides transfer functions with real poles at $s = -10$ eliminating one zero in $G_{\dot\Psi}(s)$.

Figures 4, 5, and 6 show step and frequency responses of the feed-forward control and of the single-track vehicle model for different longitudinal velocities. As intended by

Parameter	Value	Parameter	Value
ν	l	γ	l_h
EG_d	$\frac{m}{l} \cdot \left(\frac{l_h}{c_{\alpha v}} - \frac{l_v}{c_{\alpha h}}\right)$	ε	$\frac{m}{c_{\alpha h}} \cdot \frac{l_v}{l}$
k_δ	$\frac{1}{i_s}$		

Table 1. Parameters of the feed-forward control

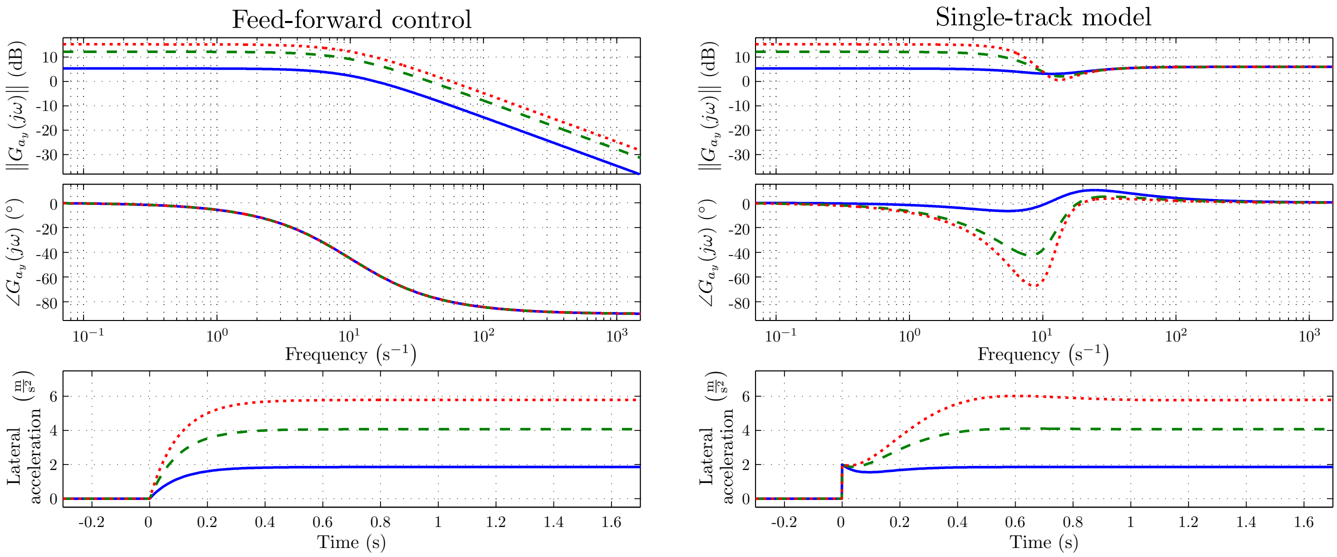

Fig. 4. Frequency and step responses of the lateral acceleration a_y for $v_{x,d} = \{$40km/h (—), 70km/h (- -), 100km/h(···)$\}$

the above choice of the free parameters the static gains and thus the final values of all regarded variables of the feed-forward control correspond to the ones of the single-track model. Nevertheless, there are remarkable differences in the transient responses.

As determined in Sec. 3.1 the dynamical behavior of the feed-forward control concerning its lateral acceleration a_y is equivalent to a first-order lag element. On the contrary, the transient response of the single-track model is not easily characterizable. Because of the relative degree $r = 0$ of its transfer function an instant increase of the lateral acceleration occurs at the time of the steering angle's step. While for higher speed the poles are dominant for small velocities the zeros dominate and thus imply an undershoot in the corresponding step response. All in all, the transient response of the lateral acceleration generated by the feed-forward control is preferable from the perspective of system theory.

Concerning the sideslip angle's behavior the feed-forward control is advantageous as well and matches the transient response of a second-order lag element with real poles mentioned above. In contrast to the single-track model its cutoff frequency and phase difference are independent of the longitudinal velocity. Moreover, its step response immediately tends towards the final value while the transient response of the single-track model shows an overshoot followed by a zero-crossing before aiming at the final value. This behavior is implied by a non-minimum phase zero in the transfer function for higher velocities which does not occur in the feed-forward control's transfer function.

Regarding the yaw rate the transient response of the feed-forward control is similar to the one of the single-track vehicle model. Furthermore, the final values coincide although the stationary yaw rate is not determined explicitly in the feed-forward control structure.

All things considered the transient response of the feed-forward control is more appealing being less dependent on the vehicle's longitudinal velocity. Furthermore, other static and dynamic behaviors can be implemented easily with the incidental parameters being arbitrary.

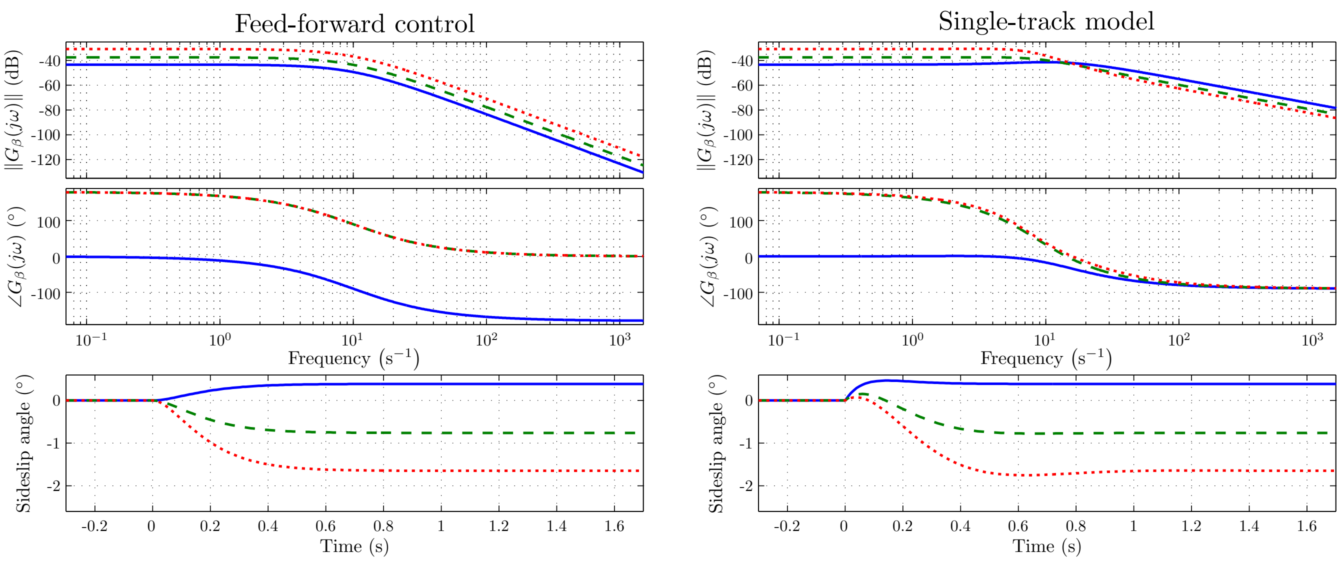

Fig. 5. Frequency and step responses of the sideslip angle β for $v_{x,d} = \{$40km/h (—), 70km/h (- -), 100km/h(···)$\}$

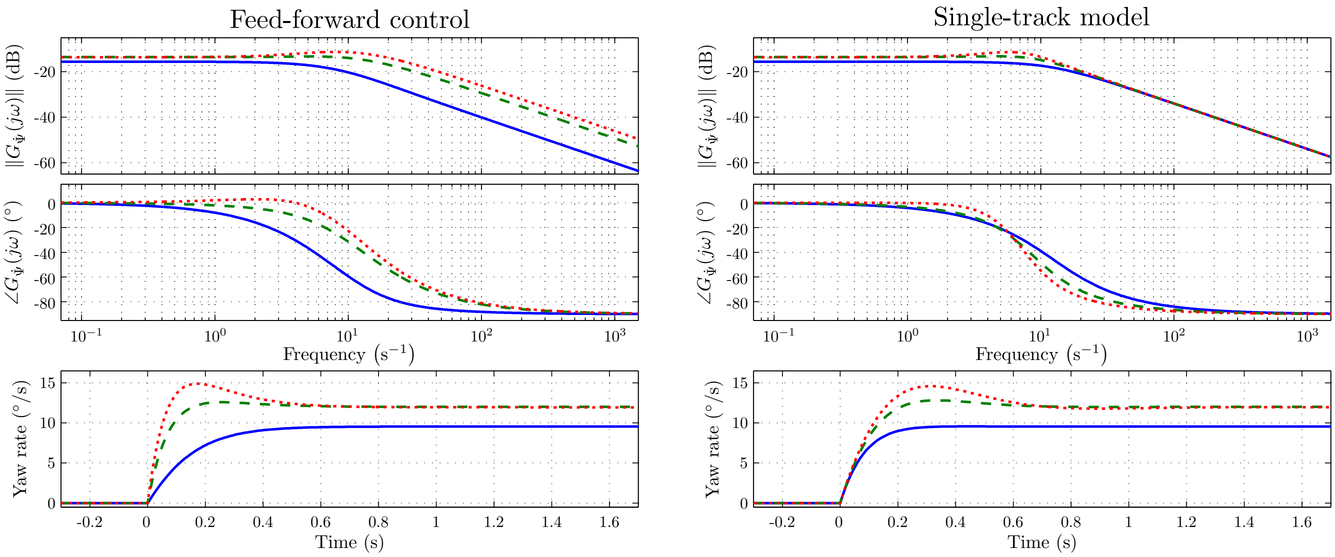

Fig. 6. Frequency and step responses of the yaw rate $\dot{\Psi}$ for $v_{x,d} = \{$40km/h (—), 70km/h (- -), 100km/h(···)$\}$

5.2 Evaluation of the tire force allocation

In this section the effectiveness of the tire force allocation derived in Sec. 4 is assessed. Therefore it is compared to an optimization based approach according to [1] which allocates the tire forces by minimizing the maximum of the four utilizations of adhesion potential $\eta_{\max}$ thus defining the dynamic optimum. In doing so a convex optimization problem is solved numerically. Furthermore, the utilization of adhesion potential of a conventional vehicle with front axle steering and fixed braking factor is looked at for comparability. Fig. 7 shows the maximum values of the four utilizations of adhesion potential resulting from the proposed analytical approach (—), the optimal force allocation (- -), and the conventional vehicle (···). As driving maneuver, a fast lane change with medium deceleration was simulated using an additional control structure so that all configurations tracked the same trajectory.

In general Fig. 7 demonstrates the potential of a vehicle with single-wheel actuators concerning safety maximization in comparison with a conventional vehicle. Furthermore, it can be stated that the proposed tire force allocation achieves similar results as the optimization based method. At the same time the computational effort is 90% less regarding the simulation duration because no numerical minimization is needed.

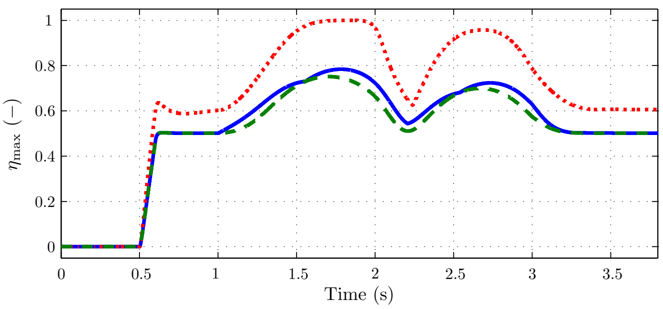

Fig. 7. Maximum value $\eta_{\max}$ of the utilizations of adhesion potential

6. CONCLUSIONS

This article presented a structured and analytical approach to generate desired trajectories and appendant tire forces for a vehicle with single-wheel actuators. First, a model-based feed-forward control for the horizontal dynamics determining a desired sideslip angle behavior and a desired self-steering behavior was developed. Subsequently, an analytical approach to allocate the required forces and moments on the chassis to the tire forces was described. The resulting control structure demonstrated its effectiveness in appropriate computer simulations.

REFERENCES

[1] R. Orend. Vehicle dynamics feedforward control with optimal utilisation of the adhesion potentials of all four tyres (German). *at-Automatisierungstechnik*, 53(1):20-27, 2005.

[2] C. Knobel, A. Pruckner, and T. Bünte. Optimized Force Allocation. *Proceedings of the 4th IFAC Symposium on Mechatronic Systems*, pp. 366–371, 2006.

[3] P. Reinold and A. Trächtler. Closed-loop control with optimal tire-force distribution for the horizontal dynamics of an electric vehicle with single-wheel chassis actuators. *Proceedings of the 2013 ACC*, pp. 2159–2164, 2013.

[4] J. Hoedt and U. Konigorski. Integrated electric vehicle control by differential parameterization. *Proceedings of the 50th IEEE CDC-ECC*, pp. 2517–2522, 2011.

[5] T.D. Gillespie. *Fundamentals of Vehicle Dynamics*. SAE, Warrendale, PA, 1992.

[6] J.-E. Moseberg and G. Roppenecker. Horizontal Vehicle Motion Control with Single-Wheel Chassis Actuators (German). *at-Automatisierungstechnik*, 62(3):216-225, 2014.

[7] A. Ben-Israel and T.N.E. Greville. *Generalized Inverses*. Springer, New York, 2003.

[8] J.-E. Moseberg and G. Roppenecker. Analytical Wheel Force Allocation for the Horizontal Dynamics of a Vehicle with Single-Wheel Chassis Actuators (German). *VDI-Berichte No. 2196*, pp. 431–436. VDI-Verlag GmbH, Düsseldorf, 2013.